Isothermal membrane-based air dehumidification: A comprehensive review

Ming Qu, Purdue University; Omar Abdelaziz, Oak Ridge national laboratory; Zhiming Gao, Oak Ridge national laboratory; Hongxi Yin, Washington University at St. Louis

ABSTRACT

Isothermal membrane-based air dehumidification (IMAD), a recent emerged air dehumidification technology, separates the moisture from the humid air by using a selective membrane, through which only vapor molecules can transfer from the one side of the membrane at a high concentration to the other side at a low concentration. The IMAD process has superior performance potentially in energy and economic than other traditional dehumidification technologies. This paper comprehensively reviews the literature on IMAD including membrane characteristics, membrane configuration, membrane-related mass transport mechanism, and system design and operation, as well as the mass transfer modeling. State of the art in the IMAD is presented and finally the recommendations of future research are provided.

Keywords: Isothermal, membrane, dehumidification, vacuum

Contents

1 INTRODUCTION

Air dehumidification is a process of removing moisture from the humid air for indoor thermal comfort, preventing mold growth, and enhancing building durability. It directly impacts the building energy consumption, the individual productivity, and health of the occupants [1]. In current practices, air dehumidification is typically done by using the two methods: condensing moisture and desiccant absorption.

More than 90% of air dehumidification systems now are based on condensing moisture to dehumidify the humid air. As shown in Fig. 1a, the condensing based air dehumidification first cools the humid air, indicated as outdoor air (OA), to its dew point, then to the dew point of the supply air (SA) along a saturation curve. The water vapor in the humid air is removed by the condensation process. The overcooled air at the dew point of SA needs be heated to the desired temperature of the SA. Therefore, condensing-based air dehumidification requires inefficient overcooling and reheating, which in turn significantly reduces the system efficiency and increases energy consumption and associated cost.

The desiccant absorption based air dehumidification uses desiccant materials, which have a high affinity for water, in contact with the humid air absorbing the moisture. It includes solid Desiccant Wheel Dehumidification (DWD) and liquid desiccant dehumidification (LDD) systems. The DWD exchanges the humidity between the process air and a waste air stream or return air via a wheel coated with a desiccant. It cannot remove all the moisture required by its own due to the limited energy available for recovery from the return air. Therefore, DWD typically works with a condensing based dehumidification system together to fulfill dehumidification [2-4], as shown in Figure 1b. The LDD systems, as shown in Fig.1c, use liquid desiccant to absorb the vapor in the humid air as indicated in 3a and 3a'. Since the absorption gives off heat to air, to achieve the desired temperature, a cooling process is needed. The cooling can be provided by vapor compression cooling or the sensible energy wheel as indicated in 3b, or 3b" in Fig. 1c. In order to reuse the desiccant, a regeneration process is needed in which the moisture absorbed by the desiccant will be removed by the thermal inputs. Therefore, only if free energy is available for the desiccant dehumidification, the desiccant dehumidification could reduce energy consumption for dehumidification [7].

Researchers have explored alternatives to these conventional air dehumidification methods to reduce energy consumption and improve indoor air quality. Interests on this is very high as the large number of U.S. DOE recent awarded projects in 2010-2015 are related to air dehumidification. Isothermal membrane-based air dehumidification (IMAD) is a new promising alternative recently developed. It is a thermodynamically efficient gas separation process [8], which is widely applied in areas of food processing, water treatment, electrochemistry, air drying, and gas separation [9-13]. It separates the vapor from the air by the drive of chemical gradient, as shown in 4a or 4a' of Fig. 1d. IMAD does not need overcooling and reheating required in condensing dehumidification, nor heat inputs to the regeneration for the desiccant dehumidification. It has superior energy and economics performance than the conventional dehumidification methods [14].

The objective of the paper is to succinctly summarize current state of knowledge on the IMAD for the researchers to create a complete understanding of IMAD by discussion the findings presented in recent research on the IMAD. To reach the goal, first, state of the

art of the IMAD process and the working principle is presented, followed by the characteristics and configurations of the membranes used in the IMAD systems. Then, the paper provides a detailed assessment of system design, modeling, and performance. It is concluded by a discussion of the research needs in the future.

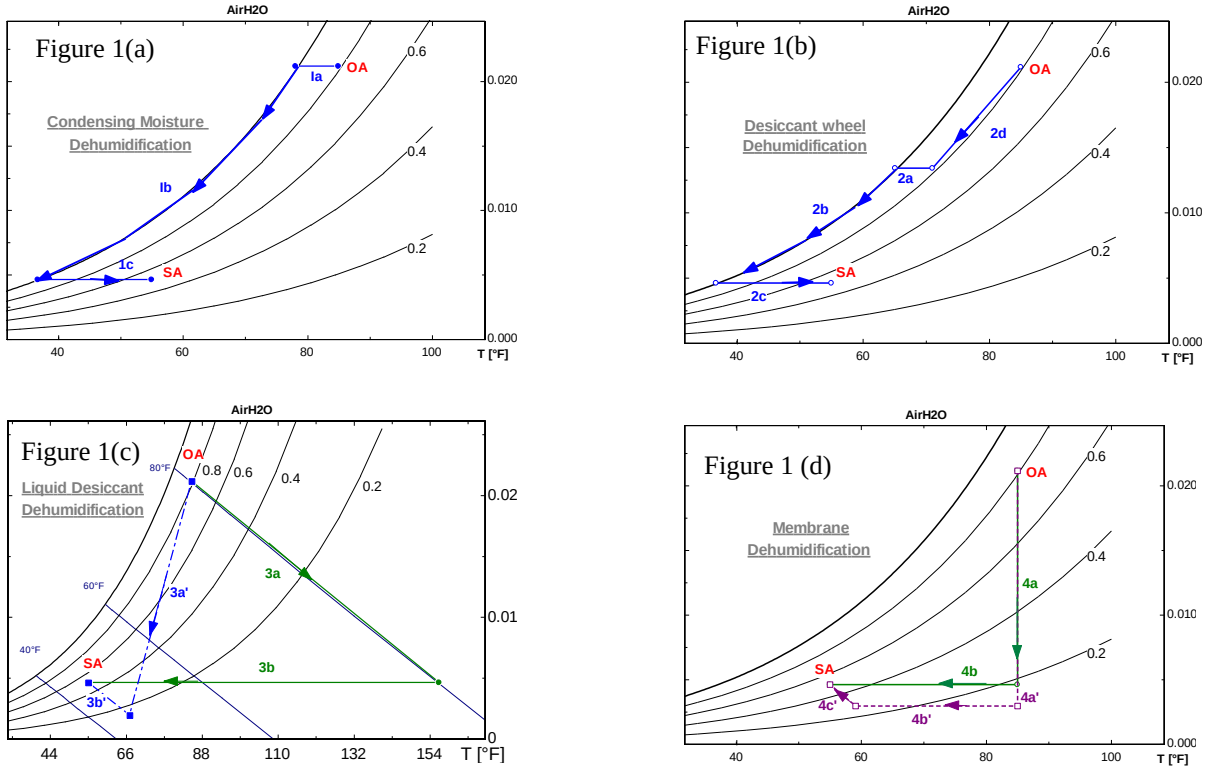

Fig. 1. Air dehumidification technology comparison a) Condensing moisture b) Desiccant wheel c) liquid Desiccant, and d) isothermal membrane-based Dehumidification

2 STATE OF THE ART OF IMAD

Membrane in the IMAD is a selective layer allowing some certain components to pass through but stops others, resulting in separating the components from the mixture. The membranes used for IMAD separates vapor gas from the humid air. The driving force for vapor transfer is the chemical potential gradient between the feed side and the permeate side of the selective membrane [15-21]. As indicated in Fig.2 of schematic diagram of IMAD, the vapor of the humid air of the feed stream, is selectively transported to the permeate side and released as the permeate and the rest of the air as the retentate stream is out for space cooling.

The permeability and selectivity are two critical characteristics that determine the vapor separating performance of the IMAD [8, 20]. Permeability is the rate at which vapor permeates through a membrane per unit area or per unit driving force. A membrane of the IMAD with a high permeability to the vapor allows the vapor to pass more rapidly than the other gas. It enables same separation with less surface area. Selectivity is the ratio of the permeability coefficient of vapor and the others

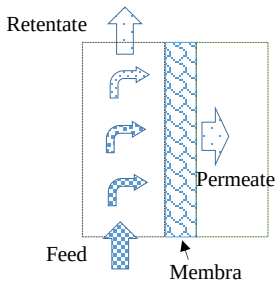

Fig. 2. Schematic diagram for IMAD

in the humid air through the membrane. A membrane with a high selectivity allows vapor only to pass through the membrane, resulting in pure water vapor in the permeate side [8]. For air dehumidification, the purity of permeated vapor is not highly required. Based on the findings from Bui et al., the IMAD can result in energy savings by using a relative low selective membrane with no requirement of a high purity [20]. Xing et. al [8] also predicted that a 50% or higher energy efficiency gain over a conventional vapor compression system was attainable when the selectivity for water vapor to air was above 200, which is much lower than the selectivity level used in gas separation application. Additionally, the membrane for IMAD should be resistant to air contamination, mechanical erosion, and bacteria attachment and growth in warm and humid air environment, as well as cost-effective to achieve better performance [21].

3 THE MEMBRANE IN IMAD

3.1 Membrane types

All the membranes have porous in spite of different sizes. According to the size of porous, the membranes used in IMAD can be divided into two types of dense and porous. Typically, the dense membranes have pores sized at the order of 0.1nm, while the porous membranes have pores at the order of 0.1 μm [24]. Except the size of porous in the membrane, the internal structure and arrangement of the porous is also used to category the type of membranes. Accordingly, membranes can be grouped in two categories: symmetrical or asymmetrical types [22]. A symmetrical membrane is uniform in composition, structure, and pore sizes. On other hand, an asymmetrical membrane is chemically or physically heterogeneous asymmetric. To maximize the productivity, membranes are typically constructed with the goal of minimizing their thickness and maximizing their area. Therefore, membranes are usually either asymmetric or composite to minimize the thickness.

3.2 Membrane materials

The materials used for in the membranes of IMAD include four main categories: polymeric, zeolitic, mixed matrix, and supported liquid.

3.2.1 Polymer membranes

The polymer membranes are the most widely used vapor permeation membranes because they are inexpensive, defect-free, reproducible, and physically robust. Among them, the hydrophilic organic polymers such as cellulose acetate (CA), ionic polymers, polyvinylalcohol (PVA), polysulfone (PSF), and polyacrylonitrile [25,26], are generally selected because the hydrophilic function in these polymer chain enhances the water solubility in the membrane. The diffusion of water molecules, therefore, is faster than the diffusion of other gases. Table 1 summaries the permeability and selectivity for 19 polymer membranes used for vapor permeation in the drying of natural gas and compressed air, and humidity control, given by Metz et al. [21]. Among them, CA and PSF were reported as the materials used for a humidity control study by El-Dessouky et. al. [27], in which the selectivity values of the CA and PSF studied were around 400, much smaller than 24000 and 8000 reported by Metz et. al. [21].

Table 1. Polymer membranes for vapor permeation [21]

Water vapor and N_2 permeability and selectivity for various polymers at 30 ˚C, extrapolated to 0 water vapor activity

Polymer	Abbreviation	H_2O Permeability (Barrer)	Selectivity (H_2O/N_2)
Ethyl cellulose	EC	20000	6061
Cellulose acetate	CA	6000	24000
Natural rubber	NR	2600	299
$1000_{PEO}56_{PBT}44$	PEO-PBT	85500	40500
Polyacrylonitrile	PAN	300	1875000
Polyamide 6 (Nylon 6)	PA-6	275	11000
Polycarbonate	PC	1400	4667
Polydimethylsiloxane	PDMS	40000	143
Polyethersulfone	PES	2620	10480
Polyethylene	PE	12	6
Polyimide (Kapton)	PI	640	5333333
Polyphenyleneoxide	PPO	4060	1068
Polypropylene	PP	68	227
Polystyrene	PS	970	388
Polysulfone	PSF	2000	8000
Polyvinylalcohol	PVA	19	33333
Polyvinylchloride	PVC	275	12500
Sulfonated polyetheretherketon	SPEEK	61000	10166667
Sulfonated polyethersulofon	SPES	15000	214286

Where, Barrer is gas permeability specific to oxygen permeability. 1 Barrer = 10^{-11} (cm^3 O_2) cm /cm^2. s. mmHg

3.2.2 Zeolitic membranes

The zeolite membranes are one type of inorganic membranes used in vapor permeation. They are thermally and chemically stable and provide better separation performance because of the crystalline inorganic framework structures with uniform, molecular-sized pores. The pores are built from aluminum, oxygen, and silicon with alkali or alkaline-earth metals such as sodium, potassium, and magnesium, plus water molecules trapped in the gaps between them [29-31].

Zeolitic typically are not self-supported, so that they grow on porous support materials like aluminum or stainless steel. Zeolite can grow to form a continuous film either by the method called in-situ or by the method of seeded. The seeded method has been preferred because it often offers greater flexibility in controlling the orientation of the zeolite crystals and the micro-structure of the zeolite membrane, but it is very expensive due to additional processing steps. Xing et. al. [8] used a combination of the in-situ and seeded methods to developing their membrane for air dehumidification by first coating a Ni sheet as the support with small seeding crystals of the targeted zeolite framework and then contacting it with a growth solution composed of NaOH, AlO3, and sodium silicate to grow by the in-situ method. To reduce the production cost of zeolite membranes, Zhang et. al. from Pacific Northwest National Laboratory, developed a low-cost, inorganic membrane module by using a hydrothermal membrane growth method to fabricate a membrane of a thin NaA zeolite on a flexible porous Ni substrate, and successfully demonstrated its use for wate and ethanol separation [32].

3.2.3 Mixed matric membranes

The mixed matrix membrane (MMM) hybrids the polymer membrane and zeolite membrane. It has a better reproducibility, an easier and cheaper fabrication process, a better transport properties and higher thermal and chemical stability. The MMM is a type of organic-inorganic nanocomposite membranes in which nanoparticles are dispersed in polymeric films. The mixed matrix membrane (MMM) hybrids the polymer membrane and zeolite membrane. It has a better reproducibility, an easier and cheaper fabrication process, a better transport properties and higher thermal and chemical stability. Both the polymer and the inorganic fillers are selective to water vapor in the humid air, but the inorganic fillers typically have significantly higher selectivity than the neat polymer. This hybrid improves membrane selectivity significantly.

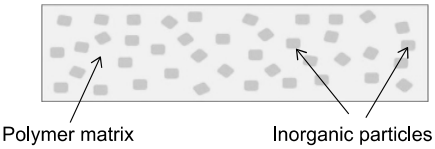

Fig. 3. Schematic representation of mixed matrix membranes [37]

A few researchers investigated the performance of MMM for vapor permeation. Cheng et al. used the gelatin-silica and PVA to fabricate a MMM for separating vapor from the mixture of propylene and the vapor. The silica-based MMM was reported to achieve a seven-time higher vapor permeance and a 14-time higher separation factor simultaneously [38]. Zhou et al. fabricated the polyurethane/TiO_2 or SiO_2 nanohybrid membranes and found the nanohybrid MMM materials showed two times higher water vapor permeability than the pure polyurethane membranes, especially under thermal stimulation [39]. Bui et al. fabricated a MMM by dipping a twilled Dutch weave stainless steel mesh scaffold, fine and porous TiO_2, in a hydrophilic solution of polyvinyl alcohol and lithium chloride at various ratios. The measured data showed that the membrane had a selective factor of 450 for vapor to air [20].

3.2.4 Supported liquid membrane

The supported liquid membrane (SLM) is designed to immobilize a liquid phase within a porous support membrane through capillary forces [40,41]. It typically includes two major layers: a single laminate of a supported liquid membrane of a hygroscopic liquid like triethylene glycol, polyethylene glycol 400, or ionic liquids, and a highly hydrophobic microporous membrane [42-47], as shown in Fig. 4. The liquid is usually stabilized in the support membrane by either direct immersion or a vacuum setting. The vacuum construction maintains a vacuum on the permeate side of the liquid membrane. Since the rate of vapor diffusion in liquids was reported to be at least three to four times higher than in polymeric membranes, the SLM could improve vapor fluxes and selectivity [48]. A recently developed ionic liquid-based liquid membranes demonstrated a vapor permeability of 26,000–46,000 Barrer and a separation factor over 1000 in Ito et al.'s work [46].

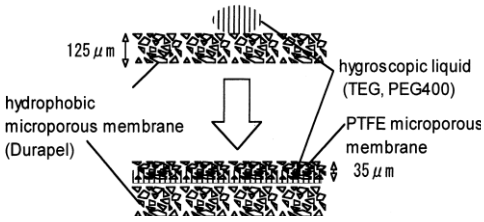

Fig. 4. The construction of the supported liquid membrane [49]

3.3 Membrane module

The membrane materials are typically constructed in the form of flat-sheets or hollow tubes as the modules used in IMAD [24,25, 51]. The configuration of the flat-sheet membrane module is similar to the typical plat-and-frame heat exchanger. The feed flow and the permeate flow is separated by the membrane sheets in a counter-flow pattern as shown in Fig. 5a. On the other hand, the hollow tubular membrane module is similar to a shell-and-tube heat exchanger as shown in Fig. 5b. The feed flow and the permeate flow are separated by the membrane tubes in a cross-flow pattern. The tubular multichannel form is preferred in commercial applications because the circular shape of the tubes enables the module to sustain a larger pressure drop across the membrane than a flat shape. The feed side could be either tube side or shell side. However, according to Scovazzon et al., feeding the process air to the tube side could result in a large pressure drop [50]. While feeding the process air to the shell side can lessen the pressure drop, the flow of the air might be distributed poorly and uneven, which in turn could result in reduced performance [52,53,54]. To make the distribution uniform, a structured arrangement of fibers on the shell side was investigated by researchers to achieve better performance [7,50].

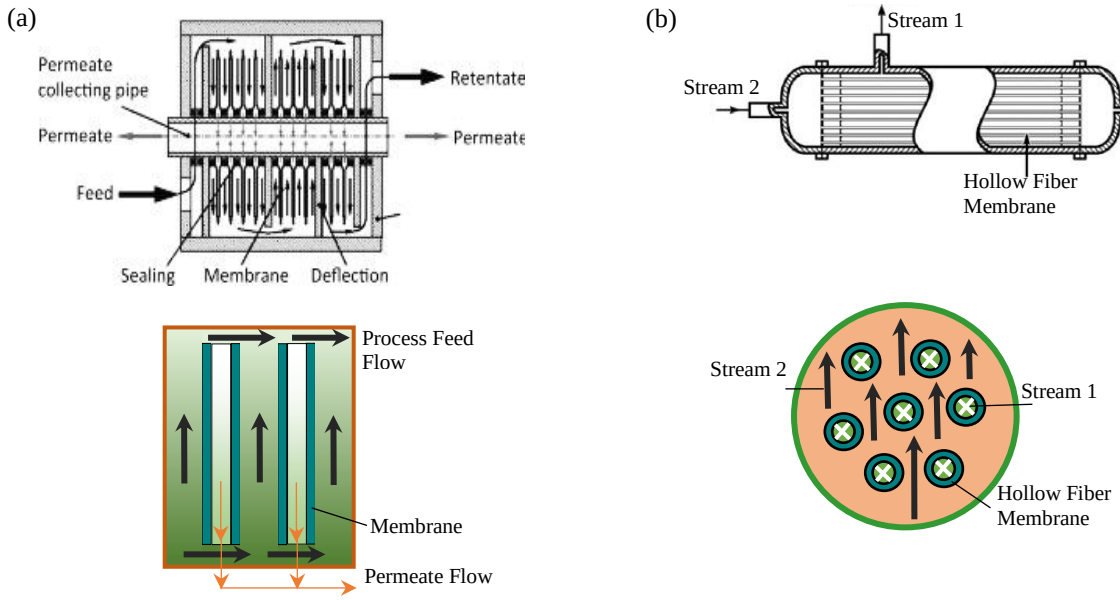

Fig. 5. Membrane modules a) flat-sheet [55] and b) tubular module

Membrane durability is one of challenges that IMAD has. IMAD inheritably has fouling issue. The life of the membrane is influenced by the environmental conditions and pollutants.

4 IMAD SYSTEM DESIGN AND OPERATION

4.1 IMAD system configuration

The IMAD system uses chemical gradient, namely the concentration or pressure gradient between two surfaces of the membrane, to drive the vapor out of humid process air across

the membrane to the permeate side. Three distinct techniques in practices are used to create the partial vapor pressure difference: feed compression (FC), vacuum pumping (VP), and gas sweep (GS) [56]. As shown in Fig.6a, FC uses a compressor to increase the pressure in the feed side while VP, indicated in Fig.6b, uses a vacuum pump to reduce the pressure at the permeate side. Both FC and VP requires energy to produce either higher or lower pressure. Different from them, GS, as depicted in Fig. 6c, adds an inert gas to the permeate side for the diluting, resulting in a lower partial vapor pressure. GS operates the permeate side at a higher total pressure and requires an additional compound like inert gas, nitrogen, or air, which can be costly. Some IMAD systems employ the combination of VP and GS, as shown in Fig. 6d, however, the combination increases energy costs and should be discarded [49,57].

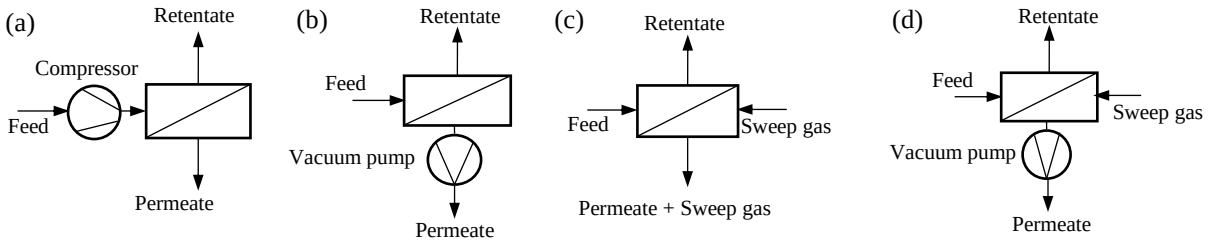

Fig. 6. Four IMAD configurations to generate the driving force on permeate side a) feed compression, b) vacuum pumping, c) gas sweep, and d)the combination of vacuum pumping and gas sweep

Additionally, VP is systematically preferable when a high purity of permeate is required [57]. Since IMAD is a new application for membrane, all the related literature found were laboratory work, among which more than 50% employed VP [8,20,27,49,59,60]; a few studies used GS system configuration as reported by Metz et al [21]; and the most of the others used the combination of VP and GS [46,50].

4.2 IMAD system design

IMAD systems is isothermal filtration without heat inputs. The only energy used in the process is the power consumption for the compressor or the vacuum pump. Since VP is most preferred and popular configuration, it is used to illustrate how the IMAD is designed and operated to remove vapor in the humid air. Typically, the desired humidity of the supply air in HVAC systems is same as the humidity of a dew point temperature at 13°C (55°F), which has a partial vapor pressure at 1.5 kPa. Therefore, the partial vapor pressure at the permeate side pressure in a VP system theoretically must be lower than 1.5 kPa. This is the most of VP systems operate the permeate side less than 1kPa, usually produced by a vacuum pump. The vacuum is used to compress air at 1kPa to an atmospheric pressure at 101 kPa, so that the work, W, required by the vacuum pump can be found as Eq. 1

$$W = \frac{nRT}{\varepsilon} ln \frac{P_{outlet}}{P_{inlet}} \qquad \text{Eq. 1}$$

where, n is the total moles of the mixture vacuumed by the pump, R is the gas constant, T is the absolute temperature, typically P_{outlet} is the atmospheric pressure, P_{inlet} is the permeate pressure, and ε is the efficiency of the vacuum pump, which can be assumed as 0.65 [8,50]. The compression ratio of the vacuum pump, $\frac{P_{outlet}}{P_{inlet}}$, determines the

magnitude of the work. To reduce energy requirement from the vacuum pump, an alternative design was devised by Dais Analytic Corporation for vacuum pumping IMAD system [24] as shown in Fig. 7. The system has a vacuum pump located between two membrane modules. The low-pressure side of the vacuum pump was designed at lower than 1.25 kPa from the permeate side of the first membrane module and the high-pressure side of the vacuum pump is at 3.5 kPa, which is the feed side of the second membrane. In this configuration, the vacuum pump does not need to compress the permeate side of the first membrane up to the ambient pressure, but at a much lower pressure at 3.5 kPa. Thus, the work used for the vacuum pump is only about one third of the work used for a typical compression ratio at 100 because the much smaller compression ratio of 3-5.

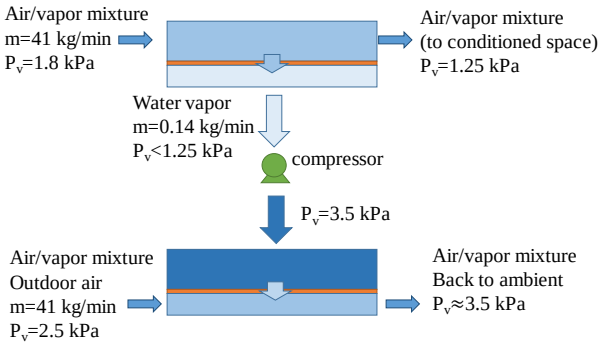

Fig. 7. Schematic diagram of alternative system design by Dais Analytic. [24]

4.3 IMAD system flow organization

Except for the partial vapor pressure, the organization of the flows also play an important role in the system efficiency. There are four ways to organize the flows and directions of the air: a) perfect mixing with two fans in both feed and permeate sides, b) cross-plug flow with the feed stream perpendicular to the permeate stream, c) co-current flow with the feed and permeate streams at same direction, and d) counter-current flow with the feed and permeate streams in opposite direction, as indicated in Fig. 8. The cross-plug flow with a reasonable precision is typically hollow-fiber membrane modules when the permeate pressure is low enough. On the other hand, a counter-current flow generally is used in flat-sheet modules [58].

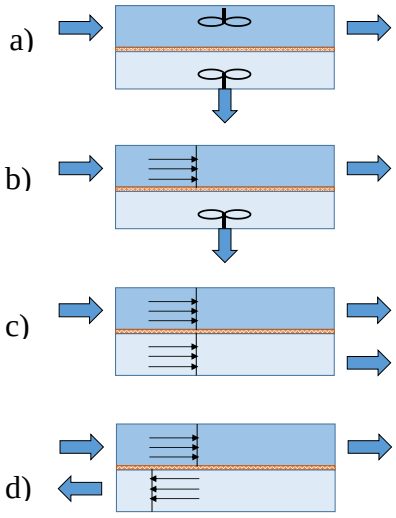

Fig. 8 Flow configurations for membrane-based dehumidification: (a) perfect mixing, (b) cross- plug flow, (c) co-current flow, and (d) counter-current flow. (Favre, 2010)

5 IMAD SYSTEM PERFORMANCE

5.1 System performance indicators

The dehumidification performance and dehumidification COP are considered the two indicators for evaluating the performance of IMAD [20]. The dehumidification performance is defined as the percentage of moisture removed as shown in Eq. 2.

$$\%\, moisture\ removed\ = \frac{\omega_{in}-\omega_{out}}{\omega_{in}} * 100\% \qquad \textit{Eq. 2}$$

where ω_{in} and ω_{out} are the humidity ratios of the feed air and the retentate air.

The dehumidification COP [8,27,50], COP_{latent}, is the ratio of the latent heat associated to the vapor removed, $\dot{Q}_{latent}$ and the work, W, needed by the vacuum pump or the compressor. It can be expressed in Eq.3

$$COP_{latent} = \frac{\dot{Q}_{latent}}{W} \qquad Eq.\ 3$$

5.2 The performance IMAD Systems

There are a few of IMAD systems available in the literature. Table 2 is a summary of the system configuration, operational condition, and membrane selectivity, and system performance. Generally, the supported liquid membranes were operated at a relatively high pressure at the permeate side compared to the other three types of membranes. Based on the limited case studies, Table 2 shows that the zeolite membrane with a selectivity of 178 produced by Xing et al. exhibited the best performance with an 83.6% moisture removal and a dehumidification COP of 3.0. The MMM membrane tested by Bui et al., on the other hand, had a dehumidification COP of 2.5, but a lower moisture removal at 20%. The studies available indicated that IMAD potentially may be competitive to the conventional air dehumidification systems along with the development of membrane materials and system design.

Table 2. Membrane properties, operational conditions, and system performance in the IMAD systems

Membrane material	Permeation method	Condition T(°C) / RH	Permeate pressure (kPa)	Water permeance mol/(m^2 Pa.s)	H_2O selectivity	%moisture removal / COP_{latent}	Refer-ence
Porous Ni-supported NaA Zeolite	VP	32 / 90%	0.8	$6.8x10^{-6}$	178	83.6% / 3.0	[8]
Ionic liquid [emim][BF_4]	VP+GS	31 / 94%	6.6	$3.5x10^{-7}$	16,300	60% / 0.75	[50]
Polysulfone hollow fiber	VP	32 / 100%	4.7	$1.8x10^{-7}$	529	-	[59]
MMM PVA: LiC, TiO	VP	24 / 90%	3	$4.5\ x10^{-7}$	450	20% / 2.5	[20]
Cellulose Triacetate	VP	35 / 95%	0.28	$1.0\ x\ 10^{-6}$	/	55%/-	[60]
Triethylene glycol (TEG)	VP	22 / 72%	0.13	$7.5\ x\ 10^{-8}$	/	83% /-	[49]
Ionic liquid [emim][DCA]	VP+GS	25 / 94%	4.5	$1.6\ x\ 10^{-6}$	1000	NA	[46]
Ionic liquid [emim][ESU]	VP+GS	25 / 94%	4.5	$1.5\ x\ 10^{-6}$	1000	NA	[46]
Ionic liquid [emim][BF_4]	VP+GS	25 /94%	4.5	$1.2\ x\ 10^{-6}$	1000	NA	[46]

6 IMAD MODELING

Modeling IMAD involves a complex mass transfer process at macro-, meso-, and micro-scales. There are three basic mass transports occurring in the IMAD as shown in Fig.9.

1. Interfacial mass transport from air to the membrane side

2. Mass Transport in the membrane
3. Interfacial mass transport from the membrane side to the permeate side

The water vapor removal rate through the membrane can be calculated as Eq. 4.

$$J_{v,all} = h_{mass\_overall}(C_f - C_p) \qquad Eq.\ 4$$

where, $J_{v,all}$ is the flux of water vapor through the membrane (kmol/(m^2 s)); C_f, C_p are the bulk concentration of water vapor at the feed and permeate sides of the membrane, respectively (kmol/m^3); and $h_{mass\_overall}$ is the overall mass transfer coefficient (m/s), which can be determined according to the three basic mass transfer coefficients (m/s) in the feed boundary layer, h_{mass_f}, the membrane, h_{mass_m}, and the permeate boundary layer h_{mass_p} ,respectively, as shown in Eq.5.

$$\frac{1}{h_{mass\_overall}} = \frac{1}{h_{mass\_f}} + \frac{1}{h_{mass\_m}} + \frac{1}{h_{mass\_p}} \qquad Eq.\ 5$$

According to the related literature, the simplified modeling for the mass transport used empirical equation or experimental data to estimate the mass transfer coefficients [61-63]. After the governing equations are determined, discretizing the governing equations in the flow direction through a one-dimensional finite-difference technique is the general common approach used to predict the behavior and performance of the IMAD [64-66]. In the method, typically a segment-by-segment methodology is used to simplify the equations in a matrix. The matrix can be solved by using Gaussian Elimination or other search route to finally identify the unknown parameters.

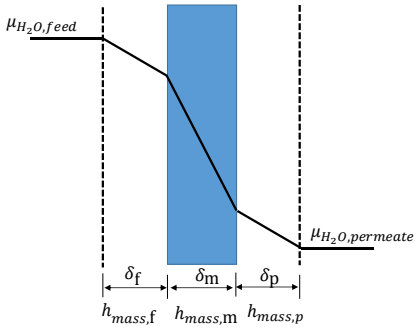

Fig. 9. the mass transfer in the stagnant boundary layers and the membrane for a vapor/air mixture

The following sections are the review on the three mass transport mechanisms and how to calculate those mass transfer resistances.

6.1 Interfacial mass transfer in feed and permeate sides of the membrane

Concentration polarization is the emergence of concentration gradients at the interface of some membranes with high selectivity [21], especially the very high flux membranes used in the processes for the separation of gas/vapor mixtures and in high pressure applications [67]. Concentration polarization is generally caused by the ability of a membrane to transport some species more readily than the others, so that the retained species are concentrated at the upstream membrane surface while the concentration of transported species decreases [68]. Fig. 9 shows the concentration polarization phenomena that occurs in the humid air if the diffusion of water vapor is through a stagnant layer on both the feed and permeate sides of the membrane. The mass transfer coefficients on the feed, h_{mass_f} and permeate sides of the membrane, h_{mass_p}can be calculated by using $\frac{Sh*D_{AB}}{L_c}$, *where,* Lc is the hydraulic diameter on the feed/ permeate side; D_{AB} is the mass diffusivity in the humid air, the calculation for which can be found in Lüdtke et al.'s work [67]; Sh is the Sherwood number, a dimensionless number. It is a function of the Reynolds number and the Schmidt number, and geometry and flow conditions. For

laminar flow conditions, Sh can be calculated either theoretically or experimentally. For turbulent flow conditions, the only method is empirical functions [67].

6.2 Mass transfer in the membrane

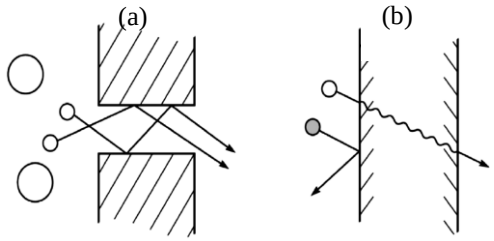

Fig. 10. Two types of membrane separation mechanisms: a) pore-flow filtration, b) solution-diffusion [23]

The mechanisms of the mass transfer in the membrane of IMAD can be grouped to two broad categories: pore-flow and solution-diffusion. In the solution-diffusion, the vapor in the humid air dissolves in the membrane as in a liquid and then diffuses through the membrane down a lower concentration permeate side due to the difference in the solubility and diffusivity of the vapor in and through the membrane material, as depicted in Figure 10b. In the pore-flow filtration, the vapor molecules in the moisture air are small enough to flow through some of the pores in the membrane to the permeate side while the majority of the other gases larger than the pores are sieved and stay in the feed side as indicated in Figure 10a. The solution-diffusion occurs in the membranes with a few or no pores. Comparably, pore-flow filtration occurs in the porous membrane, which has more and larger-sized pores. According to Baker et al [23], if the pores in a membrane are less than 0.5 nm in diameter, the mass transportation shall be modeled by using the solution-diffusion and if the pores in a membrane are greater than 1 nm in diameter, pore-flow should be used for the mass transfer. Therefore, the mass transport in the dense polymer membranes of the IMAD is based on the solution-diffusion and the other three types like zeolite membranes, MMMs, and supported liquid membranes with the selective porosity are based on the pore-flow filtration.

6.2.1 The driving force in the membrane of the IMAD

Based on thermodynamics, the driving forces producing movement of vapor in the gradient in its chemical potential. Therefore, the flux of vapor, Jv, is described by Eq. 6.

$$\mathrm{J_v} = -\mathrm{L_v}\frac{\mathrm{du_v}}{\mathrm{dx}} \qquad \text{Eq. 6}$$

Where, $\frac{du_v}{dx}$ is the gradient in chemical potential and Lv is a coefficient of proportionality linked to the chemical potential. For the IMAD, the chemical potential gradient only is related to concentration and pressure, as expressed in Eq. 7

$$du_v = RTln(r_v c_v) + v_v dp \qquad \text{Eq.7}$$

where, c_v is the molar concentration of vapor, $r_v$is the activity coefficient linked to concentration, p is the pressure in the membrane, and $v_v$is the molar volume of vapor. According to Wijmans and Baker[69], the three assumptions can be made for modeling the mass transfer in the IMAD:

1) The fluids on either side are in equilibrium with the membrane at the interface;

2) For the solution-diffusion, the pressure in a membrane is uniform and a concentration gradient is the only drive for the mass transport, as shown in Fig. 11a;

3) For the pore-flow filtration, the concentrations of solvent and solute within a membrane are uniform and the pressure gradient is the only drive for the mass transfer, as shown in Fig. 11b.

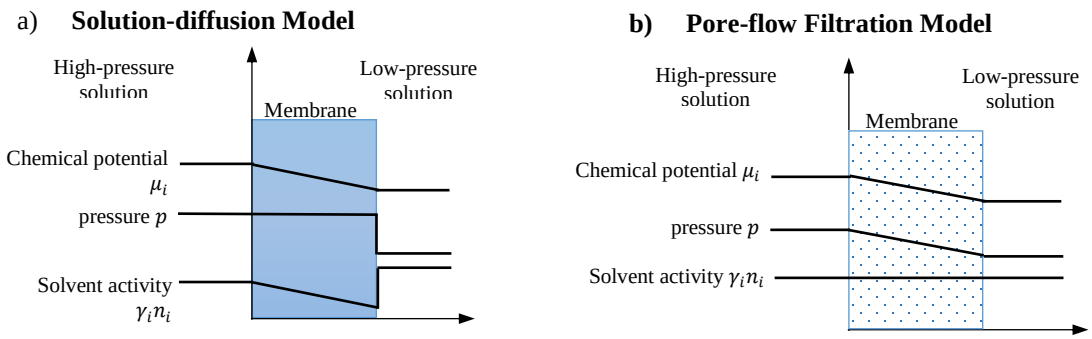

Fig.11. Permeation of a one-component solution through a membrane according to a) solution-diffusion and b) pore-flow transport reproduced by referring to [70]

6.2.2 Mass transfer in the dense membrane based on the solution-diffusion

If a IMAD uses the dense membrane, the mass transport can be derived by using the solution-diffusion model. As mentioned in the front, the mass transport in the dense membrane was driven by only the concentration gradient across the membrane and the chemical potentials on either side of the interface of gas and membrane are equal [71,72]. According to Eq. 6 and 7, the flux of vapor could be identified by using the difference of the partial pressure of vapor and the permeability coefficient of the membrane, P_i^G, as shown in Eq. 9 [71].

$$J_v = \frac{P_v^G.(p_{vf} - p_{vp})}{l} \qquad \textit{Eq. 9}$$

Where, p_{vf} and $p_{vp}$is the partial pressure of vapor in the feed and permeate streams. The permeability coefficient must be known to find the mass transfer. The cup method is the method most frequently used to determine the permeability coefficient [73]. There are other methods used to obtain the permeability coefficient to prevent the errors caused by concentration polarization [74, 21]. Alternatively, the permeability coefficient can be achieved according to the sorption coefficient and the diffusion coefficient [75].

6.2.3 Mass transport in the porous membrane based on the pore-flow filtration

6.2.3.1 Single gas permeation

For a membrane with a high selectivity in the range of 460-30000, the single gas permeation was used for analysis by neglecting air permeation [64].

As stated in the front, the mass transport through a porous membrane is driven only by pressure gradient. Combining Eq.6 and 7, in the absence of a concentration gradient in the porous membrane gives Eq. 10.

$$J_v = -\mathrm{L_v} v_v \frac{dp}{dx} \qquad \textit{Eq. 6}$$

The mass transfer in the porous membrane is complex and can be divided into four independent mechanics as follows [76, 92, 93].

1) Knudsen-diffusion, in which the pore size, d_p is so small that collisions between vapor molecules can be ignored compared to collisions of vapor molecule with the inside walls of porous membrane when the size of vapor, d_s, is smaller than the pore size, which is less than the average free path length of vapor, λ ($d_s < d_p < \lambda$);

2) Molecular-diffusion, in which molecule-molecule collisions dominate over molecule-wall collision when the average free path length of vapor is less than the pore size ($\lambda < d_p$);
3) Poiseuille flow, in which the gas behaves as a continuous fluid driven by pressure gradient. In this case, molecule-molecule collisions dominate over molecule-wall collision when the average free path length of vapor is less than the pore size ($\lambda < d_p$);
4) Molecular sieving transport when the size of vapor is almost same as $d_s \approx d_p$

The molecular-diffusion are dominated by the interaction of the transported molecular, but the real molecular diffusion coefficient, $D_{v,m}$, is reduced by the ratio of porosity, ε and tortuosity, τ. The molecular diffusion coefficient, D_{md} can be found by Eq. 10. [94]

$$D_{md} = \frac{\varepsilon}{\tau} D_{v,m} \qquad \text{Eq.10}$$

By applying kinetic gas theory to a single, straight, and cylindrical pore, the coefficient of Knudsen diffusion can be derived as Eq. 11, according to Mason et.al. [93]

$$D_{Kd} = \frac{d_p}{3} . \frac{\varepsilon}{\tau} \sqrt{\frac{8RT}{\pi M_v}} \qquad \text{Eq.11}$$

Mv is the molecular weight of vapor (kg/kmol). Therefore, the Knudsen diffusion flux can be calculated by using Eq. 12.

$$J_{v,k} = -\frac{D_{Kd}}{RT} \frac{dp_v}{dx} \qquad \text{Eq.12}$$

where Jv,k is the mass transfer rate of the Knudsen diffusion (kmol/m^2 s); dp_v/ dy is the gradient of the partial vapor pressure;

The Poiseuille flow exists when the pore size is larger than the mean free path. For a single capillary, the Poiseuille flow can be calculated by Eq. 13.

$$J_{v,p} = \frac{p_v}{RT} \frac{\varepsilon}{\tau} \frac{{d_p}^2}{32} \frac{dp}{dx} \qquad \text{Eq.13}$$

where, p is the total pressure of the air in the membrane.

If the pore diameter approach the range of the sizes of the molecules, the molecular sieving transport flux can be expressed by Eq. 14 [84]

$$J_{v,ms} = -\frac{1}{RT} \frac{\varepsilon}{\tau} D_v^c \frac{dp_v}{dx} \qquad \text{Eq.14}$$

D_v^c is the diffusion factor (m^2/s) and it can be calculated by using Eq. 15.

$$D_v^c = \rho_v . d_p . \sqrt{\frac{8\mathrm{RT}}{\pi . M_v}} e^{-\left(\frac{E_v^c}{\mathrm{RT}}\right)} \qquad \text{Eq. 15}$$

where, E_v^c is activation energy of diffusion (kJ/kmol)

For the porous membrane with different sized porous, a single or combined transport mechanisms can be used to model [18, 77-80]. Table 3 gives the mass transfer lux equations for the cases with the combined mass transport mechanisms.

6.2.3.2 Permeation in binary vapor and air in porous Membranes

Water vapor is a strongly adsorbing component and air is a weakly-adsorbing component. For such gas mixtures, many researchers studied different possible binary gas models for gas separation including adsorption–diffusion [85], the Maxwell–Stefan theory [86], and the bi-modal pore diffusion [87]. Those models, however, are not appropriate for

IMAD. To identify a better model, Van de Graaf et al. developed a simplified binary transport model based on the Maxwell–Stefan theory for a binary mixture like air and successfully verified their model by experimental data for zeolite membrane [88].

Table 3. The the mass transfer lux for the combinations of various flows [93]

Transport mechanism	The mass transport flux in (kmol/m^2 s)
Knudsen diffusion + molecular diffusion	$J_{v,kd\_md} = -\frac{D_{v,eff}}{RT}\frac{dp_v}{dx}$ Eq. 16 where, $D_{v,eff} = \frac{1}{\frac{1}{D_{kd}}+\frac{1}{D_{md}}}$ Eq.17
Knudsen diffusion + molecular Diffusion + Poiseuille flow	$J_{v,kd\_md\_pf} = J_{v,p} + J_{v,kd\_md}$ Eq.18

Xing et al. confirmed that the binary transport model is principally suitable for modeling of the IMAD [8]. The following is a simple introduction to the Maxwell–Stefan theory, which is the basis for the mass transfer in the multi-gases mixtures. The assumption made in the Maxwell_Stefan theory is that a driving force for the movement of a species is balanced by the frictions among the moving species and their surroundings [89-91]. The generalized form of this equation is expressed as Eq. 19.

$$-\frac{\nabla \mu_i}{RT} = \sum_{\substack{j=1 \\ j\neq i}}^{j=n} \frac{x_j J_i - x_i J_j}{C_t D_{ij}},\ i = 1,2,\ldots..,n \qquad \textit{Eq. 7}$$

where, μ_i is the chemical potential of species i (kJ/kmol); x_i, x_j is the molar fraction of species i and j; Ji and Jj are the molar flux for i and j (kmol/ s); D_{ij} is the Maxwell_Stefan diffusivity (m^2/s) and represents inverse friction factor between molecules i and j. c_t is the total molar concentration of the fluid mixture (kmol/m^3). More details on how to use the Maxwell_Stefan theory in Zeolite or MMM porous membranes can be found in [80].

7 CONCLUSIONS AND REMARKS FOR FUTURE IN IMAD

Isothermal membrane-based air dehumidification, a recent emerged air dehumidification technology, separates the moisture from the humid air by using a selective membrane. Through IMAD only vapor molecules can transfer from the one side of the membrane at a high concentration to the other side at a low concentration. The IMAD process has superior performance in energy and economic than other traditional dehumidification technologies. This review provides a comprehensive discussion of the IMAD technology including the membrane materials and characteristics, membrane forms and modules, system configuration and operation, and mass transport modeling. The key discussions in the paper can be summarized as:

- The four types of membranes used in IMAD include polymeric, zeolitic, mixed matrix, and supported liquid. According to the existing literatures, zeolitic and mixed matrix membranes have shown better performance for air dehumidification. Between the two typical membrane modules of flat-sheets and hollow tubes, the tubular module is usually preferred in commercial applications. Feeding the process air to the tube side could result in a large pressure drop, while feeding the process air to the shell side can lessen the pressure drop, but air is distributed poorly and uneven.

- Three distinct techniques used in IMAD to create the partial vapor pressure difference are feed compression, vacuum pumping, and gas sweep. More than 50% of IMAD system in the literature employed vacuum pumping.
- The only energy used in the IMAD is the power consumption for the compressor or the vacuum pump. Placing a vacuum pump located between two membrane modules can reduce the compression ratio of the vacuum pump, which results in the improvement of the dehumidification COP of IMAD.
- Four ways to organize the flows and directions of the air in the IMAD are 1) perfect mixing, 2) cross-plug flow, 3) co-current flow, and 4) counter-current flow. The cross-plug flow is typically used in hollow-fiber membrane modules while a counter-current flow generally is used in flat-sheet modules.
- The dehumidification COP is the ratio of the latent heat associated to the vapor removed and the work needed by the vacuum pump or the compressor. Among the studies in the literature available, the zeolite membrane has the highest moisture removal and the dehumidification COP. And the IMAD with the best performance achieved an 83.6% moisture removal and a dehumidification COP of 3.0.
- The three basic mass transports in the IMAD include 1) interfacial mass transport from air to the membrane side; 2) mass transport in the membrane; and 3) interfacial mass transport from the membrane side to the permeate side.
- The mechanisms of the mass transfer in the membrane of IMAD can be grouped to pore-flow and solution-diffusion. The dense membrane-based IMAD can be modeled by using a solution-diffusion model, in which the pressure in a membrane is uniform and a concentration gradient is the only drive for the mass transport. For the porous membranes, the pore flow filtration should be used to estimate the diffusions. In the pore flow diffusion, the concentrations of solvent and solute within a membrane are uniform and the pressure gradient is the only drive for the mass transfer.
- Air dehumidification in the IMAD have been modeled as a single gas permeation in some literatures. The mass transfer of a single permeation in the porous membrane can be divided into four independent mechanics: 1)Knudsen-diffusion; 2)molecular-diffusion; 3)poiseuille flow; and d)molecular sieving transport depending upon the pore size of the membrane.
- Water vapor is a strongly adsorbing component and air is a weakly-adsorbing component. For such gas mixtures, many researchers modeled it as binary gas in the process of gas separation including adsorption–diffusion, the Maxwell–Stefan theory, and the bi-modal pore diffusion.
- Membrane durability is one of challenges that IMAD has. IMAD inheritably has fouling issue. The membrane degrades due to the environmental conditions and pollutants.

Currently, IMAD technology is new and in the research phase. It still lacks knowledge of system performance, familiarity, optimal design and system analysis to achieve significant energy savings, low energy consumption, and low operational cost. The technology is immature for the implementation on industrial scale compared to other well-established air dehumidification technologies. Important advances must be made in IMAD technology if it is to be widely used in air dehumidification. Several research, therefore, are highly

needed to understand the technology and address its environmental, economic, and energy impacts.

The development of membrane material and module

- The membranes used for gas separation and drying applications shall be carefully studied for the development of the IMAD's membrane to achieve better system performance. New materials of membrane with high water permeability and selectivity are needed for better dehumidification performance. The materials must be inexpensive, strong enough to sustain the pressure, and no/less degrading.
- New membrane modules that possess better mass transport than the existing module designs need to be studied and developed. The new developed membrane module should address the challenges of the durability, the deformation, and the maldistribution. Balance must be found among the moisture removal, the dehumidification COP, and the cost during the selection of membrane and the design of the pressure difference.

Advancement of system optimal design, operation, and control

- IMAD must be coupled with the air conditioning process for comfortable indoor conditions.
- System energy performance models are highly needed for identification of the best system design, operation, and control to minimize energy consumption, the impacts from the operating parameters, and the maintenance and operational system cost, while to achieve high energy efficiency and overall system COP.
- Environmental and economic assessment is a valuable investigation to assist people in making a decision compared to other air dehumidification technologies.

Application of IMAD for large-scale systems

- All the IMAD studies in the literature were based on laboratory scale experimentation. Large-scale systems are still scarce. Membrane modules, system configuration, capacity, operation, and control for scale-up systems shall be investigated to reduce the size, pressure drop while to enhance heat and mass transfer.
- Practical challenges, such as the aging and degradation properties and fouling, should be explored.

8 ACKNOWLEDGEMENTS

This work was supported by the U.S. Department of Energy Oak Ridge Energy Laboratory under Contract No. DE-EE000704.

9 REFERENCE

[1] Harriman III, L. G., Plager, D. & Kosar, D., 1997. Dehumidification and cooling loads from ventilation air. ASHRAE Journal, p. 37 – 45.

[2] Rambhad, K. S., Walke, P. V. & Tidke, . D., 2016. Solid desiccant dehumidification and regeneration methods—A review. Volume 59, pp. 73-83.

[3] La, D. et al., 2010. Technical development of rotary desiccant dehumidification and air conditioning: A review. Volume 14, pp. 130-147.

[4] O'Connor, D., Calautit, J. K. S. & Hughes, B. R., 2016. A review of heat recovery technology for passive ventilation applications. Volume 54, pp. 1481-1493.

[5] Yin, Y., Qian, J. & Zhang, X., 2014. Recent advancements in liquid desiccant dehumidification technology. Volume 31, pp. 38-52.

[6] Sultan, M. et al., 2015. An overview of solid desiccant dehumidification and air conditioning systems. Volume 46, pp. 16-29.

[7] Kneifel, K. et al., 2006. Hollow fiber membrane contactor for air humidity control: Modules and membranes. Journal of Membrane Science, 276 (1–2), pp. 241-251.

[8] Xing, R. et al., 2013. Advanced thin zeolite/metal flat sheet membrane for energy efficient air dehumidification and conditioning. Chemical Engineering Science, 104(18), pp. 596-609.

[9] Zaw, K., Safizadeh, M. R., Luther, J. & Ng, K. C., 2013. Analysis of a membrane based air-dehumidification unit for air conditioning in tropical climates. Applied Thermal Engineering, 59(1-2), pp. 370-379.

[10] Criscuoli, A., Carnevale, M. C. & Drioli, E., 2016. Study of the performance of a membrane-based vacuum drying process. Separation and Purification Technology, Volume 158, pp. 259-265.

[11] Berk, Z., 2013. Chapter 10 - Membrane Processes. In: Food Process Engineering and Technology. San Diego: Academic Press, pp. 259-285.

[12] Ang, W. L., Mohammad, A. W., Hilal, N. & Leo, C. P., 2015. A review on the applicability of integrated/hybrid membrane processes in water treatment and desalination plants. Volume 363, pp. 2-18.

[13] Tien, H. T. & Ottova-Leitmannova, A., 2000. Chapter 6 Membrane electrochemistry. In: Membrane Science and Technology. s.l.:s.n., pp. 283-348.

[14] Pan, F. et al., 2008. P(AA-AMPS)–PVA/polysulfone composite hollow fiber membranes for propylene dehumidification. Journal of Membrane Science, Volume 323, pp. 395-403.

[15] Neel, J., 1991. Introduction to Pervaporation in: Pervaporation Membrane, Separation Process. Amsterdam: Elsevier.

[16] Charcosset, C., 2011. Downstream processing and product recovery/membrane systems and technology. Comprehensive Biotechnology, Volume 2, p. 603–618.

[17] Chiam, C.-K. & Sarbatly, R., 2013. Vacuum membrane distillation processes for aqueous solution treatment—A review. Volume 74, pp. 27-54.

[18] Alkhudhiri, A., Darwish, N. & Hilal, N., 2012. Membrane distillation: A comprehensive review. Volume 287, pp. 2-18.

[19] Strathman, H., 2011. Membranes and membrane separation processes. 1 Principles. Volume 22, p. 413–454.

[20] Bui, T. D., Chen, F., Nida, A. & Chu, K. J., 2015. Experimental and modeling analysis of membrane-based air dehumidification. Separation and Purification Technology, 144(15), pp. 114-122.

[21] Metz, S. et al., 2005. Transport of water vapor and inert gas mixtures through highly selective and highly permeable polymer membranes. Journal of Membrane Science, 251(1-2), pp. 29-41.

[22] Baker, R. W., 2001. Membrane Technology. s.l.: Encyclopedia Of Polymer Science and Technology.

[23] Baker, R. & Low, B., 2015. Membrane Separation. s.l.: Elsevier - In Reference Module in Chemistry, Molecular Sciences and Chemical Engineering.

[24] Woods, J., 2014. Membrane processes for heating, ventilation, and air conditioning. Volume 33, pp. 290-304.

[25] Bolto, B., Hoang, M., Gray, S. & Xie, Z., 2015. Chapter 9 - New generation vapour permeation membranes. In: Pervaporation, Vapour Permeation and Membrane Distillation. Oxford: Woodhead Publishing, pp. 247-273.

[26] Murali, R. S., Sankarshana, T. & Sridhar, S., 2013. Air separation by polymer-based membrane technology. Volume 42, p. 130–186.

[27] El-Dessouky, H., Ettouney, H. & Bouhamra, W., 2000. A Novel Air Conditioning System: Membrane Air Drying and Evaporative Cooling. Chemical Engineering Research and Design, 78(7), pp. 999-1009.

[28] Okamoto, K., Kita, H., Horii, . K. & Tanaka, K., 2001. Zeolite NaA membrane: Preparation, single-gas permeation, and pervaporation and vapor permeation of water/organic liquid mixtures. Industrial & Engineering Chemistry Research, Volume 40, p. 163.

[29] Woodford, C., 2009. Zeolites. Available at: http://www.explainthatstuff.com/zeolites.html [Accessed 21 2 2016].

[30] Zhang, Y. et al., 2012. Hydrogen-selective zeolite membrane reactor for low temperature water gas shift reaction. Chemical Engineering Journal, Volume 197, pp. 314-321.

[31] Kosinov, N., Gascon, J., Kapteijn, F. & Hensen, E. J., 2016. Recent developments in zeolite membranes for gas separation. Volume 499, pp. 65-79.

[32] Zhang, J. & Liu, W., 2011. Thin porous metal sheet-supported NaA zeolite membrane for water/ethanol separation. Journal of Membrane Science, 371(1-2), pp. 197-210.

[33] Freeman, B., Yampolskii, Y. & Pinnau, I., 2006. Materials Science of Membranes for Gas and Vapor Separation. United States: John Wiley & Sons.

[34] Chung, T.-S., Jiang, L. Y., Li, Y. & Kulprathipanja, S., 2007. Mixed matrix membranes (MMMs) comprising organic polymers with dispersed inorganic fillers for gas separation. Progress in Polymer Science, 32(4), pp. 483-507.

[35] Aroon, M., Ismail, A., Matsuura, T. & Montazer-Rahmati, M., 2010. Performance studies of mixed matrix membranes for gas separation: A review. Separation and Purification Technology, 75(3), pp. 229-242.

[36] Sanchez, C., Belleville, P., Popall, M. & Nicole, L., 2011. Applications of advanced hybrid organiceinorganic nanomaterials: From laboratory to market. Chemical Society Reviews, Volume 40, pp. 696-753.

[37] Wolińska-Grabczyk, A. & Jankowski, A., 2015. 6 - Membranes for vapour permeation: preparation and characterization. In: Oxford: Woodhead, pp. 145-175.

[38] Cheng, Q., Pan, F., Chen, B. & Jiang, Z., 2010. Preparation and dehumidification performance of composite membrane with PVA/gelatin–silica hybrid skin layer. Journal of Membrane Science, 363(1-2), pp. 316-325.

[39] Zhou, H. et al., 2008. The polyurethane/SiO2 nano-hybrid membrane with temperature sensitivity for water vapor permeation, Journal of Membrane Science. 318(1-2), pp. 71-78.

[40] Scovazzo, P., 2010, Testing and evaluation of room temperature ionic liquid (RTIL) membranes for gas dehumidification, Journal of Membrane Science, 355(1–2), pp. 7-17.

[41] Vandezande, P., 2015. 5 - Next-generation pervaporation membranes: recent trends, challenges and perspectives. In: Woodhead Publishing Series in Energy. Oxford: Woodhead Publishing, pp. 107-141.

[42] Krull, F., Medved, M. & Melin, T., 2007. Novel supported ionic liquid membranes for simultaneous homogeneously catalyzed reaction and vapor separation. Chemical Engineering Science, 62(18-20), pp. 5579-5585.

[43] Lozano, . L. J., Godinez, C. & De los Rios, A. P., 2011. Recent advances in supported ionic liquid membrane technology. Journal of Membrane Science, Volume 376, pp. 1-14.

[44] Malik, M. A., Hashim, M. A. & Nabi, F., 2011. Ionic liquids in supported liquid membrane technology. Chemical Engineering Journal, Volume 171, pp. 242-254.

[45] Grünauer, J. et al., 2015. Ionic liquids supported by isoporous membranes for CO2/N2 gas separation applications. Journal of Membrane Science, 494(15), pp. 224-233.

[46] Kudasheva, A., Kamiya, T., Hirota, Y. & Ito, A., 2016. Dehumidification of air using liquid membranes with ionic liquids. Volume 499, p. 379–385.

[47] Asfand, F. & Bourouis, M., 2015. A review of membrane contactors applied in absorption refrigeration systems. Volume 45, pp. 173-191.

[48] Ong, Y. T., Yee, K. F., Cheng, Y. K. & Tan, S. H., 2014. A review on the use and stability of supported liquid membranes in the pervaporation process. Separation and Purification Reviews, Volume 43, pp. 62-88.

[49] Ito, A., 2000. Dehumidification of air by a hygroscopic liquid membrane supported on surface of a hydrophobic microporous membrane. 175(35-42).

[50] Scovazzo, P. & Scovazzo, A. J., 2013. Isothermal dehumidification or gas drying using vacuum sweep dehumidification. Applied Thermal Engineering, 50(10), pp. 225-233.

[51] Camacho, L. et al., 2013. Advances in membrane distillation for water desalination and purification applications. Water, Volume 5, pp. 94-196.

[52] Wickramasinghe, S., Semmens, M. J. & Cussler, E., 1992. Mass transfer in various hollow fiber geometries. Journal of Membrane Science, 69(3), pp. 235-250.

[53] Chen, H. et al., 1998. Experimental velocity measurements and effect of flow maldistribution on predicted permeator performances. Journal of Membrane Science, Volume 139, p. 259–268.

[54] Lipscomb, G. & Sonalkar, S., 2004. Sources of non-ideal flow distribution and their effect on the performance of hollow fiber gas separation modules. Separation & Purification Reviews, Volume 33, p. 41–76.

[55] Melin, T. & Rautenbach, R., 2007. Membranverfahren – Grundlagen der Modul- und Anlagenauslegung. s.l.:Springer.

[56] Harlacher, T. & Wessling, M., 2015. Chapter Thirteen - Gas–Gas Separation by Membranes. In: Progress in Filtration and Separation. Oxford: s.n., pp. 557-584.

[57] Vallieres, C. & Favre, E., 2004. Vacuum versus sweeping gas operation for binary mixtures separation by dense membrane processes. Journal of Membrane Science, 244(1-2), pp. 17-23.

[58] Favre, E., 2010. 2.08 - Polymeric Membranes for Gas Separation. In: Comprehensive Membrane Science and Engineering. Oxford: Elsevier, pp. 155-212.

[59] Auvil, S. R., Choe, J. S. & Kellogg, L. J., 1993. US, Patent No. 5259869.

[60] Pan, C., Jensen, C., Bielech, C. & Habgood, H., 1978. Permeation of water vapor through cellulose triacetate membranes in hollow fiber form. Volume 22, p. 2307–2323.

[61] Zhang, L.-Z., 2011(a), Heat and mass transfer in a randomly packed hollow fiber membrane module: A fractal model approach. International Journal of Heat and Mass Transfer, Volume 54, p. 13–14.

[62] Charfi, K., Khayet, M. & Safi, M., 2010. Numerical simulation and experimental studies on heat and mass transfer using sweeping gas membrane distillation. Desalination, 259(1-3), pp. 84-96.

[63] Karanikola, V. et al., 2015. Sweeping gas membrane distillation: Numerical simulation of mass and heat transfer in a hollow fiber membrane module. Journal of Membrane Science, Volume 483, pp. 15-24.

[64] Zhang, L. & Jiang, Y., 1999. Heat and mass transfer in a membrane-based energy recovery ventilator. Journal of Membrane Science, Volume 163, pp. 29-38.

[65] Bergero, S. & Chiari, A., 2001. Experimental and theoretical analysis of air humidification/dehumidification processes using hydrophobic capillary contactors. Applied Thermal Engineering, 21(11), pp. 1119-1135.

[66] Woods, J. & Kozubal, E., 2013. A desiccant-enhanced evaporative air conditioner: Numerical model and experiments. Energy Conversion and Management, Volume 65, pp. 208-220.

[67] Lüdtke, O., Behling, R.-D. & Ohlrogge, K., 1998. Concentration polarization in gas permeation. Journal of Membrane Science, 146(2), pp. 145-157.

[68] Strathmann & H., 2004, Ion-Exchange Membrane Separation Processes. Amsterdam: Elsevier.

[69] Paul, D., 1974. Diffusive Transport in Swollen Polymer Membranes. In: Permeability of Plastic Films and Coatings. New York: Plenum Press, pp. 35-48.

[70] Wijmans, J. & Baker, R., 1995. The solution-diffusion model: a review. 107(1-2), pp. 1-21.

[71] Wijmans, J. G. & Baker, R. W., 2006. The Solution–Diffusion Model: A Unified Approach to Membrane Permeation. In: Materials Science of Membranes for Gas and Vapor Separation. s.l.:Wiley.

[72] Baker, R. W., 2004. Membrane Transport Theory, in Membrane Technology and Applications. In: Membrane Technology and Applications. Chichester: John Wiley & Sons.

[73] ASTM, 2012. ASTM E96: Standard Test Methods for Water Vapor Transmission of Materials, s.l.: American Society for Testing and Materials.

[74] Stroeks, A., 2001. The moisture vapour transmission rate of block copoly(ether-ester) based breathable films. 2. Influence of the thickness of the air layer adjacent to the film. Polymer, Volume 42, pp. 9903-9908.

[75] Min, J., Hu, T. & Liu, X., 2010. Evaluation of moisture diffusivities in various membranes. Journal of Membrane Science, 357(1-2), pp. 185-191.

[76] Seidel-Morgenstern, A., 2010. Membrane Reactors. Weinheim: Wiley-VCH.

[77] Curcio, E. & Drioli, E., 2005. Membrane distillation and related operations - A review. Separation and Purification Reviews, 34(1), pp. 35-86.

[78] Essalhi, M. & Khayet, m., 2015. 10 - Fundamentals of membrane distillation. In: Woodhead Publishing Series in Energy. Oxford: Woodhead Publishing, pp. 277-316.

[79] Burggraaf, A., 1996. Chapter 9 Transport and separation properties of membranes with gases and vapours, Fundamentals of Inorganic Membrane Science and Technology. Elsevier, pp. 331-433.

[80] Cengel, Y. & Ghajar , A., 2010. Heat and Mass Transfer: Fundamentals and Applications. 4 ed. s.l.:McGraw-Hill Science/Engineering/Math.

[81] Nagy, E., 2012. On Mass Transport Through a Membrane Layer. In: Basic Equations of the Mass Transport through a Membrane Layer. OxforD: Elsevier, pp. 1-34.

[82] Gates, D., 1980. Biophysical ecology. New York, Heidelberg, Berlin: Springer Verlag.

[83] Uhlhom, R. & Burggraaf, A., 1990. Gas separation with inorganic membranes. In: Inorganic Membranes. New York: s.n., pp. 155-176.

[84] Thomas, S., Schafer, R., Caro, J. & Seidel-Morg, A., 2001. Investigation of mass transfer through inorganic membrane with several layers. Catalysis Today, Volume 67, pp. 205-216.

[85] Dong, J., Lin, Y. S. & Liu, W., 2000. Multicomponent hydrogen/hydrocarbon separation by MFI-type zeolite membranes. AIChE Journal, 46(10), pp. 1957-1966.

[86] Shah, D. et al., 2000. Pervaporation of alcohol–water and dimethylformamide–water mixtures using hydrophilic zeolite NaA membranes: mechanisms and experimental results. 179(1-2), pp. 185-205.

[87] Nomura, M., Yamaguchi, T. & Nakao, S.-i., 2001. Transport phenomena through intercrystalline and intracrystalline pathways of silicalite zeolite membranes. 187(1-2), pp. 203-212.

[88] Van de Graaf, J., Kapteijn, F. & Moulijn, J., 1999. Modeling permeation of binary mixtures through zeolite membranes. AIChE Journal, Volume 45, pp. 497-511.

[89] Giacinti Baschetti, M. & De Angelis, M., 2015. 8 - Vapour permeation modelling. In: Pervaporation, Vapour Permeation and Membrane Distillation. Oxford: Woodhead Publishing, pp. 203-246.

[90] Krishna, R. & Wesselingh, J., 1997. The Maxwell-Stefan approach to mass transfer. Volume 52, pp. 861-911.

[91] Amundsen, N., Pan, T. W. & Paulsen, V., 2003, Diffusing with Stefan and Maxwell. Volume 49, pp. 813-830.

[92] Ding, Z., Ma, R. , Fane, A.G., 2003, A new model for mass transfer in direct contact membrane distillation, Desalination, Volume 151, pp. 217-227

[93] Seidel-Morgenstern, A. (2010) Membrane Reactors. Wiley-VCH, Weinheim

[94] Mason, E.A., and Malinauskas, A.P. (1983) Gas Transport in Porous Media: The Dusty Gas Model. Elsevier, Amsterdam.